Aerosol absorption over the clear-sky oceans deduced from POLDER-1 and AERONET observations

Article

Published Version

Aerosol absorption over the clear-sky oceans deduced from POLDER-1 and AERONET observations

N. Bellouin,[1] O. Boucher,[1] D. Tanré,[1] and O. Dubovik[2]

Received 13 February 2003; revised 5 June 2003; accepted 10 June 2003; published 23 July 2003.

[1] We estimate aerosol absorption over the clear-sky oceans using aerosol geophysical products from POLDER-1 space measurements and absorption properties from ground-based AERONET measurements. Our best estimate is 2.5 Wm^{-2} averaged over the 8-month lifetime of POLDER-1. Low and high absorption estimates are 2.2 and 3.1 Wm^{-2} based on the variability in aerosol single-scattering albedo observed by AERONET. Main sources of uncertainties are the discrimation of the aerosol type from satellite measurements, and potential clear-sky bias induced by the cloud-screening procedure. *INDEX TERMS:* 0305 Atmospheric Composition and Structure: Aerosols and particles (0345, 4801); 1640 Global Change: Remote sensing; 3359 Meteorology and Atmospheric Dynamics: Radiative processes. **Citation:** Bellouin, N., O. Boucher, D. Tanré, and O. Dubovik, Aerosol absorption over the clear-sky oceans deduced from POLDER-1 and AERONET observations, *Geophys. Res. Lett.*, *30*(14), 1748, doi:10.1029/2003GL017121, 2003.

1. Introduction

[2] Absorption by atmospheric aerosols recently arised as an important process in the climate forcing issue. One usually distinguishes between the radiative perturbation due to all (natural and anthropogenic) aerosols, and the radiative forcing due to anthropogenic aerosols only. *Ramanathan et al.* [2001] showed that during the Indian Ocean Experiment (INDOEX) differences between the aerosol radiative perturbation at the top-of-atmosphere (TOA) and surface could reach 15–18 Wm^{-2}, due to the large absorption by Asian anthropogenic aerosol. *Ackerman et al.* [2000] suggested that this large absorption may affect the vertical profiles of temperature and relative humidity, and hence cloud formation. Similar values of aerosol absorption have been measured for biomass burning aerosols during forest fires in Indonesia [*Podgorny et al.*, 2003] and over the Mediterranean Sea [*Lelieveld et al.*, 2002]. Atmospheric absorption relates to the surface radiative budget. *Wild* [1999] emphasizes that the absence of absorbing aerosols in GCMs may be responsible for miscalculated regional surface and atmospheric radiative budgets.

[3] Atmospheric aerosols enhance the atmospheric absorption through their own absorption and by scattering incoming solar radiation, thus increasing the mean photon path and the chances of absorption by gases. Aerosol absorption is computed as the difference between the TOA and surface radiative perturbations. If the TOA direct perturbation over the clear-sky oceans has been shown to be on a global average of the order of magnitude of -5 Wm^{-2} [*Boucher and Tanré*, 2000; *Christopher and Zhang*, 2002], the surface perturbation has only been estimated locally. Using POLDER (Polarization and Directionality of the Earth's Reflectances) satellite measurements and accounting for the measured aerosol absorption, *Kaufman et al.* [2002a] estimated a ratio of 3.5 between TOA and surface perturbations over the INDOEX region, which corroborates estimates made by *Ramanathan et al.* [2001] and *Tahnk and Coakley* [2002].

[4] This study aims at giving a first estimate of aerosol absorption over the clear-sky oceans, on a global scale. Aerosol optical thickness and Ångström coefficient inverted from POLDER and aerosol radiative properties inverted from AERONET (Aerosol Robotic Network) sunphotometer measurements are used to estimate the aerosol absorption. Our work is limited to oceanic regions.

2. Radiative Transfer Calculations

2.1. POLDER Products

[5] The POLDER instrument, which flew aboard the Japanese platform ADEOS from November 1996 to June 1997, allows the retrieval of the aerosol optical thickness at 865 nm, τ, and the aerosol Ångström coefficient, α, computed between the 670 and 865 channels [*Deuzé et al.*, 2000]. Because aerosol absorption cannot be measured from POLDER, the retrieval is based on 12 pre-selected monomodal non-absorbing aerosol models, with Ångström coefficients ranging from 0 to 1.4 (Table 1).

[6] In this study, absorption is accounted for by changing the modal radius and imaginary part of the refractive index of each of the 12 models in order to adjust the single-scattering albedo (SSA), ϖ_0, to the values discussed below. The real part of the refractive index and the Ångström coefficient for scattering are not modified, as presented in Table 1 for a sample SSA of 0.89 at 670 nm. By using a constant imaginary refractive index throughout the solar spectrum, we can reproduce to a large extent the observed spectral variation in SSA. At first order, the aerosol contribution to the observed radiance is proportional to the product $\varpi_0\tau$. POLDER inversion scheme involves non-absorbing aerosol models, thus leading to the measurement of the scattering optical thickness. It is converted here to an extinction optical thickness by scaling it with a factor equal to $1/\varpi_0$.

2.2. Choice of the Aerosol Single-Scattering Albedo

[7] The selection of the single-scattering albedo at 670 nm, ϖ_0^{670}, implies the identification of the aerosol type. The

[1]Laboratoire d'Optique Atmosphérique, CNRS UMR 8518, Université des Sciences et Technologies de Lille, Villeneuve d'Ascq, France.
[2]Laboratory for Terrestrial Physics, NASA Goddard Space Flight Center, Greenbelt, Maryland, USA.

0094-8276/03/2003GL017121$05.00

Table 1. Some Aerosol Models Used in This Study

	Aerosol Modal Radius (μm)	Aerosol Effective Radius (μm)	Refractive Index	α	Modified Modal Radius (μm)	Modified Refractive Index
1	0.2710	1.72	1.33-0.0i	0.0	0.2210	1.33-0.0065i
2	0.1445	0.92	1.33-0.0i	0.3	0.1314	1.33-0.0096i
3	0.0713	0.45	1.33-0.0i	0.8	0.0674	1.33-0.0129i
4	0.0335	0.21	1.33-0.0i	1.4	0.0322	1.33-0.0131i
5	0.2239	1.42	1.40-0.0i	0.0	0.1865	1.40-0.0073i
6	0.1216	0.77	1.40-0.0i	0.3	0.1113	1.40-0.0108i
7	0.0577	0.37	1.40-0.0i	0.8	0.0577	1.40-0.0146i
8	0.0293	0.19	1.40-0.0i	1.4	0.0282	1.40-0.0152i
9	0.1815	1.15	1.50-0.0i	0.0	0.1510	1.50-0.0085i
10	0.1000	0.63	1.50-0.0i	0.3	0.0912	1.50-0.0125i
11	0.0510	0.32	1.50-0.0i	0.8	0.0482	1.50-0.0168i
12	0.0252	0.16	1.50-0.0i	1.4	0.0243	1.50-0.0179i

Aerosol models used in the POLDER retrieval schemes are given in columns 2–3. As an example, columns 5–6 present the modified modal radius and refractive index to get a single-scattering albedo of 0.89 at 670 nm without changing the value of the Ängström coefficient (column 4) and real part of the refractive index. Mie calculations are done assuming a lognormal size distribution, with a standard deviation $\sigma_0 = 0.86$. The aerosol refractive index is assumed constant over the solar spectrum.

aerosol identification algorithm is presented in Figure 1. Sea salt and dust (coarse mode aerosols) are characterized by an Ångström coefficient smaller than a threshold, α_{th}, and differentiated according to the optical thickness being smaller or larger than a threshold, τ_{th}. Here, α_{th} and τ_{th} at 865 nm are set to 0.5 and 0.3, respectively. According to the aerosol climatology built by *Dubovik et al.* [2002] from AERONET measurements, dust is not very absorptive ($\varpi_0^{670} = 0.98 \pm 0.01$ at the Cape-Verde site, where ± represents the standard deviation of the measurements) although in some cases dust-dominated aerosol exhibits larger absorption (e.g., $\varpi_0^{670} = 0.95 \pm 0.03$ at the Persian Gulf site). Sea salt is given $\varpi_0^{670} = 0.98 \pm 0.03$ from Hawaii measurements.

[8] In the presence of small aerosols (α larger than α_{th}, which happens during pollution or biomass-burning events), aerosol type identification is based on geographical location (Figure 2). The aerosol SSA applied in each box is derived from cloud-screened, daily measurements at 54 AERONET coastal sites worldwide, from 1997 to 2002. Considered retrievals have an Ångström coefficient larger than α_{th} in order to address fine mode aerosols, and an aerosol optical thickness larger than 0.2 to ensure the quality of the SSA retrieval. To be consistent with the POLDER retrieval, the Ångström coefficient is computed using the optical thicknesses measured in the 870 and 670 channels. For a given box, all sites exhibit similar absorption properties and seasonal variability. The SSA applied to a given box is then the average of the SSAs measured at each site, weighted by the measured aerosol optical thickness. Pollution aerosols are found to be absorptive, with $\varpi_0^{670} = 0.95$

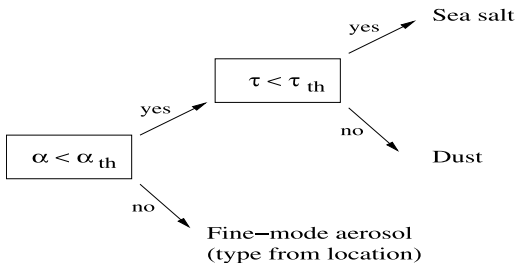

Figure 1. Algorithm used to identify the aerosol type.

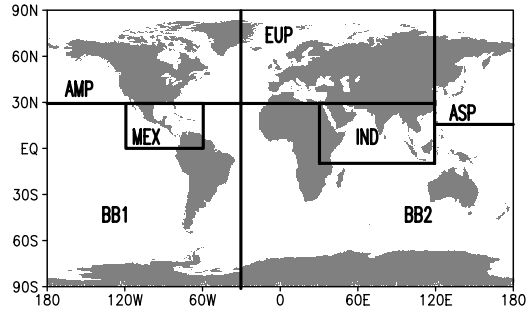

Figure 2. Definition of the boxes used in this study to choose between the fine-mode aerosol types: North-American pollution (AMP), European pollution (EUP), Mexican pollution (MEX), Asian pollution (ASP), INDOEX model (IND), South-American (BB1) and African (BB2) biomass-burning aerosol.

for North-America, 0.94 for East Asia and Europe. Measurements in the Central America area indicate quite high absorption with a SSA of 0.92. Biomass burning aerosol around Africa and Australia has been given a SSA of 0.87. Around South-America, measurements show a lower absorption, with a SSA of 0.90. For the Indian Ocean region, measurements presented by *Dubovik et al.* [2002] at the Maldives site suggest a highly absorbing aerosol, with a SSA of 0.89 ± 0.03. In order to avoid discontinuity between the boxes, a linear transition function is applied near the sides of each box.

[9] To account for the uncertainties and seasonal variabilities in measured SSA, we define three different scenarios, representing our best, low, and high estimations of the aerosol absorption. Aerosol SSAs used for each of the scenarios are summarized in Table 2. For desert dust aerosol, high absorption is obtained by choosing the Persian Gulf aerosol instead of the Cape-Verde one. Sea salt keeps the same SSA in all three scenarios, as it is expected that the large variability reported by *Dubovik et al.* [2002] is mainly due to the fact that retrieval is done at small optical thickness. Moreover, to our knowledge, the low absorption of sea-salt-dominated aerosol has not been questioned in the literature. For North-American, European, Asian, and Mexican pollution, lower and higher values of the SSA are obtained by accounting for a variability of ±0.02. INDOEX model variability has been computed to ±0.03 by *Dubovik et al.* [2002]. We get the extreme cases for biomass burning models by applying only

Table 2. Values of the Single-Scattering Albedos at 670 nm Used in This Study for Each Aerosol Type or Geographical Location

Aerosol type	Best	Low	High
Coarse mode			
Dust	0.98	0.98	0.95
Sea Salt	0.98	0.98	0.98
Accumulation mode			
North Am. Pollution	0.95	0.97	0.93
European Pollution	0.94	0.96	0.92
Mexican Pollution	0.92	0.94	0.90
Asian Pollution	0.94	0.96	0.92
INDOEX Aerosol	0.89	0.92	0.86
South Am. Biomass Burning	0.90	0.90	0.87
African Biomass Burning	0.87	0.90	0.87

The three columns correspond to the best, low, and high absorption estimates, respectively (see text for explanation of the different values).

one of the two available models to the whole southern hemisphere. Lowest absorption is obtained with the South-American model, largest with the African one.

2.3. Aerosol Radiative Perturbation

[10] For each set of 12 models, characterized by its SSA, optical properties (phase function, optical thickness and SSA) are computed using Mie theory at 24 wavelengths in the visible. TOA and surface radiative perturbations are calculated for 10 values of the solar zenith angle and for an aerosol optical thickness τ_0 of 0.1 at 865 nm. The values of the aerosol perturbations at other optical thicknesses are derived based on the fact that the perturbation is proportional to $(1\text{-}e^{-\tau})$ to a good approximation [*Boucher et al.*, 1998]. Radiative transfer calculations are performed at 24 visible bands using the Streamer radiative code [*Key and Schweiger*, 1998] with a mid-latitude summer profile for all seasons. Use of different profiles would change the results by no more than 2%. The aerosol layer is assumed to be located below 3 km. The surface reflectance is that of the open ocean and is assumed to be Lambertian, but depends on the value of the solar zenith angle. For calculation of foam and sun glint reflectances, the 10-m wind speed is taken constant at 7 ms^{-1}.

[11] When computing the aerosol radiative perturbations for each oceanic, clear-sky pixel, the values of the reference perturbations are interpolated in solar zenith angle and Ångström coefficient, but not in refractive index. The 24h-averaged aerosol perturbation (at TOA and surface) is computed as:

$$\Delta F_{day} = \int_{day} \Delta F(\tau_0, \alpha, m, \mu(t)) \frac{1 - e^{-\tau}}{1 - e^{-\tau_0}} dt / \int_{day} dt \qquad (1)$$

where $\mu(t)$ is the cosine of the solar zenith angle at time of the day t, τ, α, and m are the measured optical thickness corrected for absorption, Ångström coefficient, and refractive index retrieved at that pixel. We assume here that the daily observation of POLDER (at about 10am local time) is representative of daytime condition. This is to a large extent justified by the analysis of the intraday variability in sunphotometer aerosol optical thickness [*Kaufman et al.*, 2000]. Finally the daily aerosol radiative perturbation is gridded at a resolution of 0.5° × 0.5° before applying monthly and seasonal averaging.

3. Results and Limitations

[12] Figure 3 shows the seasonal distributions of aerosol-induced absorption. The 8-month averaged clear-sky aerosol absorption is 2.5, 2.2, and 3.1 Wm^{-2} for the 3 scenarios. These 2.5 Wm^{-2} correspond to the difference in radiative perturbation of -5.2 Wm^{-2} at the TOA and -7.7 Wm^{-2} at the surface. This translates into a ratio of 1.5 between TOA and surface perturbations. The aerosol absorption pattern is dominated by biomass-burning aerosol, mainly located in tropical regions, and fossil fuel combustion. Using the cloud-cover, *CC*, retrieved from POLDER measurements [*Buriez et al.*, 1997], we can estimate the clear-sky contribution to the total aerosol absorption as

$$\overline{A} = \overline{A_{clear}}(1 - \overline{CC}) \qquad (2)$$

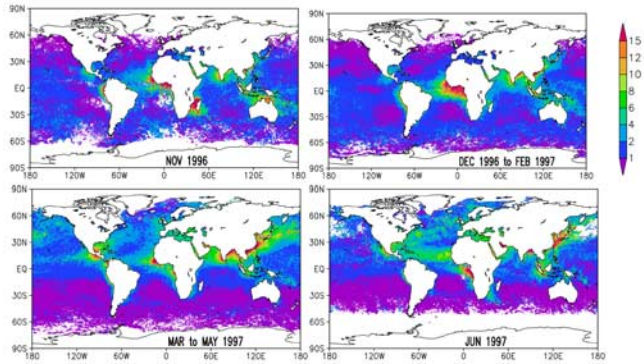

Figure 3. Distributions of the seasonally-averaged aerosol absorption (Wm^{-2}) deduced from POLDER and AERONET measurements.

where A_{clear} is the clear-sky absorption and the overline denotes monthly averaging. Aerosols also absorb in cloudy sky, so this clear-sky contribution is a lower bound to the total aerosol absorption. The 8-month averaged clear-sky contribution is 0.8 Wm^{-2}.

[13] There are of course assumptions causing uncertainties in our first-order estimation of aerosol absorption. Those uncertainties cannot be thoroughly estimated, but some limitations can be identified. The estimation of the SSAs applied to the boxes relies on thousands of AERONET measurements. For the sake of simplicity, the information on the local variability was ignored. Yet, as we considered only those retrievals done at large aerosol optical thickness, we were able to sample the actual pollution or biomass-burning event. When POLDER measurements detect an event, we are then confident that a fair value of the aerosol SSA is used.

[14] We also estimated the sensitivity of our results to the choice of our Ångström coefficient threshold. The choice of α_{th} is important as absorbing aerosols are to be found among fine-mode aerosols. For the month of March 1997, setting α_{th} to 0.4 and 0.7 instead of 0.5, aerosol absorption changes from 2.8 Wm^{-2} to 3.1 and 2.4 Wm^{-2}, respectively. As POLDER slightly underestimates the Ångström coefficient, 0.7 is an upper threshold for discriminating small and large aerosols.

[15] The cloud screening used to identify the clear-sky pixels among POLDER observations is quite robust, but may still misidentify thick dust events as clouds [*Boucher and Tanré*, 2000]. It may be necessary to go to a higher resolution than that of POLDER to allow sampling of clear-sky regions close to cloud edges. In order to compute the total aerosol absorption, one would need the vertical profile of aerosol and cloud extinction. But there is presently no remote-sensing technique capable of observing aerosols in a cloudy sky. Spaceborne lidars should allow the retrieval of aerosol layers above cloud layers.

4. Conclusion

[16] We estimated the 8-month, globally-averaged clear-sky aerosol absorption at 2.5 Wm^{-2} over oceans. Low and high absorption scenarios lead to 2.2 and 3.1 Wm^{-2}, respectively. Fine- and coarse-mode aerosols were distinguished by

applying thresholds on the aerosol Ångström coefficient. Selection among the several fine-mode aerosol types was done using geographical location. The clear-sky contribution of the aerosol absorption is estimated at 0.8 Wm^{-2} using the retrieved cloud cover. Algorithm for remote-sensing aerosol absorption from space [*Kaufman et al.*, 2002b], and forthcoming satellite instruments will soon allow a better estimate of aerosol absorption and its uncertainty.

[17] **Acknowledgments.** POLDER-1 is a joint CNES/NASDA effort. Information on the POLDER products can be found at http://smsc.cnes.fr/POLDER/. We thank the AERONET principal investigators and their staff for establishing and maintaining the 54 sites used in this study. Stefan Kinne and an anonymous reviewer are acknowledged for their constructive comments. The LOA is a member of the "fédération de recherche" of the CNRS FR1818. This research project is supported by the "Programme National de Télédétection Spatiale" (PNTS) of the CNRS.

References

Ackerman, A. S., O. B. Toon, D. E. Stevens, A. J. Heymsfield, V. Ramanathan, and E. J. Welton, Reduction of tropical cloudiness by soot, *Science*, *288*, 1042–1047, 2000.

Boucher, O., et al., Intercomparison of models representing shortwave radiative forcing by sulfate aerosols, *J. Geophys. Res.*, *103*, 16,979–16,998, 1998.

Boucher, O., and D. Tanré, Estimation of the aerosol perturbation to the Earth's radiative budget over the oceans using POLDER satellite aerosol retrievals, *Geophys. Res. Lett.*, *27*, 1103–1106, 2000.

Buriez, J.-C., et al., Cloud detection and derivation of cloud properties from POLDER, *Int. J. Remote Sens.*, *18*, 2785–2813, 1997.

Christopher, S. A., and J. Zhang, Shortwave aerosol radiative forcing from MODIS and CERES observations over the oceans, *Geophys. Res. Lett.*, *29*, 1859, doi:10.1029/2002GL014803, 2002.

Deuzé, J. L., P. Goloub, M. Herman, A. Marchand, and G. Perry, Estimate of the aerosol properties over the ocean with POLDER, *J. Geophys. Res.*, *105*, 15,329–15,346, 2000.

Dubovik, O., B. Holben, T. F. Eck, A. Smirnov, Y. J. Kaufman, M. D. King, D. Tanré, and I. Slutsker, Variability of absorption and optical properties of key aerosol types observed in worldwide locations, *J. Atmos. Sci.*, *59*, 590–608, 2002.

Kaufman, Y. J., B. Holben, D. Tanré, I. Slutsker, A. Smirnov, and T. F. Eck, Will aerosol measurements from TERRA and AQUA polar orbiting satellites represent the daily aerosol abundance and properties?, *Geophys. Res. Lett.*, *27*, 3861–3864, 2000.

Kaufman, Y. J., D. Tanré, and O. Boucher, A satellite view of aerosols in the climate system, *Nature*, *419*, 215–223, 2002a.

Kaufman, Y. J., J. V. Martins, L. A. Remer, M. R. Schoeberl, and M. A. Yamasoe, Satellite retrieval of aerosol absorption over the oceans using sunglint, *Geophys. Res. Lett.*, *29*, 1928, doi:10.1029/2002GL015403, 2002b.

Key, J. R., and A. J. Schweiger, Tools for atmospheric radiative transfer: STREAMER and FLUXNET, *Computers & Geosciences*, *24*, 443–451, 1998.

Lelieveld, J., et al., Global air pollution crossroads over the Mediterranean, *Science*, *298*, 794–799, 2002.

Podgorny, I. A., F. Li, and V. Ramanathan, Large aerosol radiative forcing due to the 1997 Indonesian forest fire, *Geophys. Res. Lett.*, *30*, 1028, doi:10.1029/2002GL015979, 2003.

Ramanathan, V., et al., Indian Ocean Experiment: An integrated analysis of the climate forcing and effects of the great Indo-Asian haze, *J. Geophys. Res.*, *106*, 28,371–28,398, 2001.

Tahnk, W. R., and J. A. Coakley, Aerosol optical depth and direct radiative forcing for INDOEX derived from AVHRR: Observations, January–March 1996–2000, *J. Geophys. Res.*, *107*, 8010, doi:10.1029/2000JD000183, 2002.

Wild, M., Discrepancies between model-calculated and observed shortwave atmospheric absorption in areas with high aerosol loadings, *J. Geophys. Res.*, *104*, 27,361–27,371, 1999.

N. Bellouin, Laboratoire d'Optique Atmosphérique, CNRS UMR 8518, Université des Sciences et Technologies de Lille, 59655 Villeneuve d'Ascq cedex, France. (bellouin@loa.univ-lille1.fr)

O. Dubovik, Laboratory for Terrestrial Physics, NASA Goddard Space Flight Center, Greenbelt, MD, USA.